Journal of the Iranian Chemical Society (2023) 20:591–597
https://doi.org/10.1007/s13738-022-02685-7

ORIGINAL PAPER

Fe_3O_4@SiO_2@Pr-Oxime-$(BuSO_3H)_3$ synthesis and its application as magnetic nanocatalyst in the synthesis of heterocyclic [3.3.3] propellanes

Zohreh Kheilkordi[1] · Ghodsi Mohammadi Ziarani[1] · Alireza Badiei[2] · Fatemeh Mohajer[1] · Rafael Luque[3]

Received: 24 July 2022 / Accepted: 29 October 2022 / Published online: 15 November 2022
© Iranian Chemical Society 2022

Abstract

The modification of Fe_3O_4 nanomagnetic particles with inorganic and organic compounds was accomplished. The Fe_3O_4@SiO_2@Pr-Oxime-$(BuSO_3H)_3$ as Brønsted acid was synthesized by functionalization of Fe_3O_4 in several steps and characterized by various techniques. Domino reaction of dimedone, anilines, ninhydrin, and malononitrile was investigated by a magnetic catalyst without using solvent at 80 °C. This method has many advantages including short reaction time, green conditions, ecofriendly, excellent yields of products, and easy separation by an external magnet.

Graphic abstract

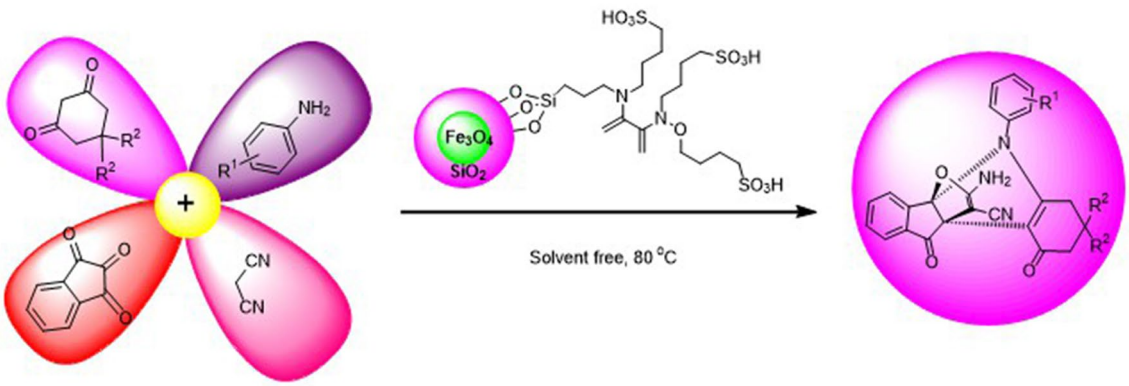

Keywords Magnetic nanocatalyst · [3.3.3]propellane · Multicomponent reaction · Fe_3O_4@SiO_2@Pr-Oxime-$(BuSO_3H)_3$ · Domino reaction

Introduction

Recently, using nanoparticles as catalysts in organic reactions has attracted many researchers. Among them, magnetic nanoparticles such as Fe_3O_4 are so important [1–3], because of their applications in many fields including drug delivery [4, 5], enzyme stabilization [6, 7], food industry [8], water refinery [9], hyperthermia [10, 11], and magnetic nanocatalyst [12–16].

Fe_3O_4 nanoparticles have various advantages including high stability, simple synthesis, low toxicity, high surface era, easy separation, and good magnetic behavior [17–19].

✉ Ghodsi Mohammadi Ziarani
gmohammadi@alzahra.ac.ir

✉ Rafael Luque
rafael.luque@uco.es

[1] Department of Organic Chemistry, Faculty of Chemistry, Alzahra University, Vanak Square, Tehran, Iran

[2] School of Chemistry, College of Science, University of Tehran, Tehran, Iran

[3] Departamento de Quimica Organica, Universidad de Cordoba, Campus de Rabanales, Edificio Marie Curie, 14014 Córdoba, Spain

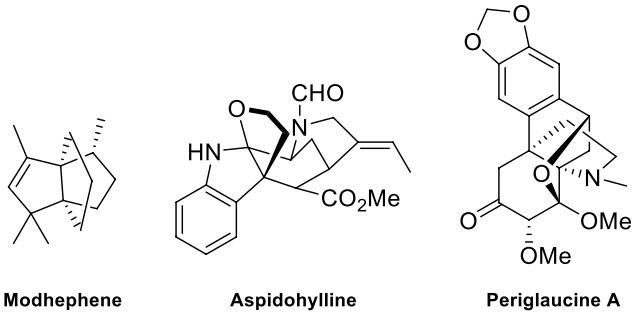

Scheme 1 Propellane skeleton in natural compounds.

Propellanes have tricyclic systems, which are joined together by a carbon–carbon single bond [20]. Propellane derivatives exist in the natural compound structures such as modhephene [21], aspidohylline [22], and periglaucine A [23, 24] (Scheme 1).

The propellanes have various properties such as anticancer [25], selective T-cell cytotoxicity [26], antibiotics [27], and antibacterial [28]. Different types of propellanes include thioxo[3.3.3]propellane, oxa[3.3.3]propellane, oxathiaza[3.3.3]propellane, and oxa*za*[3.3.3]propellane [29, 30]. Propellanes are inert toward nucleophiles, but in the presence of free radical compounds, they have high activities. Also, the [3.3.3]propellanes are found in the natural product structures [31–33].

Multicomponent reactions (MCRs) have attracted much attention due to their different advantages such as easy work-up, reduction in reaction time, simple extraction, and purification in organic chemistry [34, 35]. In the past decades, they have been applied in the synthesis of various heterocycles. Therefore, various procedures for the synthesis of propellane compounds were published by many researchers [29, 36–38]. In continuation of our previous works [39–43], the surface of Fe_3O_4 core was improved by organic reagents for the synthesis of Fe_3O_4@SiO_2@Pr-Oxime-$(BuSO_3H)_3$ as Brønsted acid. Afterward, the Fe_3O_4@SiO_2@Pr-Oxime-$(BuSO_3H)_3$ was used as a catalyst to give [3.3.3]propellanes *via* the domino reaction of anilines, dimedone, ninhydrin, and malononitrile under the solvent-free condition.

Experimental

Synthesis of Fe_3O_4, Fe_3O_4@SiO_2, and Fe_3O_4@SiO_2@Pr-NH_2

It is reported in supporting information [44, 45].

Synthesis of Fe_3O_4@SiO_2@Pr-Oxime

First, Fe_3O_4@SiO_2@Pr-NH_2 (1 g) in dry toluene (25 mL) was sonicated for 1 hour to give Fe_3O_4@SiO_2@Pr-Oxime nanoparticles. Then, 1,4-diacetyl-monooxime-one (5 mmol, 0.5 g) was added to the colloidal mix and refluxed for 36 h. Finally, by an external magnet, the magnetic nanoparticles were separated, washed with EtOH, and dried.

Fe_3O_4@SiO_2@Pr-Oxime-$(BuSO_3H)_3$ synthesis

First, Fe_3O_4@SiO_2@Pr-Oxime (1 g) in dry toluene (25 mL) was sonicated for 1 h. Then, 1,4-butane sultone (5 mmol, 5 mL) was added to the colloidal mix and refluxed for 36 h. Finally, the magnetic nanocatalyst was separated by an external magnet, washed with CH_2Cl_2, and dried.

Synthesis of [3.3.3]propellane

The reaction of dimedone (1.0 mmol, 0.14 g) and 4-bromoaniline (1 mmol, 0.16 g) by Fe_3O_4@SiO_2@Pr-Oxim-$(BuSO_3H)_3$ (0.01 g) at 80 °C after ten minutes gave enaminone, which was reacted with ninhydrin (1 mmol, 0.16 g) and malononitrile (1 mmol, 0.66 g) and stirred under the same conditions. The reaction progress was monitored by TLC in EtOAc/*n*-hexane (8:2). The reaction mixture was dissolved in hot EtOH, and the nanomagnetic catalyst was separated using an external magnet. The pure product was obtained by cooling alcoholic filtrate. The products were investigated using melting point and FTIR spectra. The NMR and mass spectra of the new compound were characterized.

(4b*R*,9b*S*)-11-((l2-azaneylidene)-l3-methyl)-12-amino-5-(3,4-dimethylphenyl)-7,8-dihydro-5H,10H-4b,9b-(epoxyetheno)indeno[1,2-b]indole-9,10(6H)-dione (5k)

Yellow powder; **m.p.** 233-235 °C; **IR (KBr, cm^{-1}):** 3418, 3342, 3229, 3184, 2962, 2942, 2920, 2191, 1717, 1636, 1596, 1502, 1435, 1391, 1323, 1271, 1218, 1188, 1017, 799. ^{1}H NMR (DMSO, 500MHz): 1.84-1.90 (m, 2H, CH_2), 2.05-2.10 (d.t, 1H, CH_2), 2.20-2.22 (t, 2H, CH_2), 2.24 (s, 3H, Me), 2.29 (s, 3H, Me), 2.42-2.49 (d.t, 1H, CH_2), 6.75-6.77 (m, 1H, Ar), 7.04-7.05 (d, 1H, Ar), 7.12 (s, 1H, Ar), 7.27-7.28 (d, 1H, Ar), 7.48 (s, 2H, NH_2), 7.63-7.66 (m, 2H, Ar), 7.84-7.86 (m, 1H, Ar). Mass (m/z)= 423 (M^+), 395, 381, 340, 350, 323, 309, 270, 254, 240, 227, 190, 177, 164, 139, 128, 103, 90, 77.

Results and discussion

Preparation of Fe_3O_4@SiO_2@Pr-Oxime-($BuSO_3H$)$_3$

First, Fe_3O_4 nanomagnetic particles were synthesized *via* the reaction of $FeCl_3.6H_2O$ and $FeCl_2.4H_2O$ in an ammonia solution (25%)/H_2O at 100 °C under a nitrogen atmosphere. Then, nanomagnetic particles were coated with tetraethyl orthosilicate at room temperature to provide Fe_3O_4@SiO_2 nanoparticles, which were modified by 3-(triethoxysilyl) propan-1-amine to provide Fe_3O_4@SiO_2@Pr-NH_2 nanoparticles, followed by the modification with 1,4-diacetylmonoxime-one *via* Schiff base reaction. Finally, the Fe_3O_4@SiO_2@Pr-Oxime nanoparticles were functionalized with acidic groups of $BuSO_3H$ *via* the reaction of the surface amine group with 1,4-butane sultone to obtain Fe_3O_4@SiO_2@Pr-Oxime-($BuSO_3H$)$_3$ (Scheme 2) [46].

Characterization of Fe_3O_4@SiO_2@Pr-Oxime-($BuSO_3H$)$_3$

The FTIR spectra of the Fe_3O_4, Fe_3O_4@SiO_2, Fe_3O_4@SiO_2@Pr-NH_2, Fe_3O_4@SiO_2@Pr-Oxime, and Fe_3O_4@SiO_2Pr-Oxime-($BuSO_3H$)$_3$ are shown in Figure 1. The Fe–O, SiO_4, and Si–O–Si group vibrations were shown at around 574 cm^{-1}, 800 cm^{-1}, and 1080 cm^{-1}, respectively. The C–H stretching vibrations of alkyl groups, acidic group (SO_3H), and OH agent in the silica shell were indicated in the area 2931 and 3442 cm^{-1}, respectively.

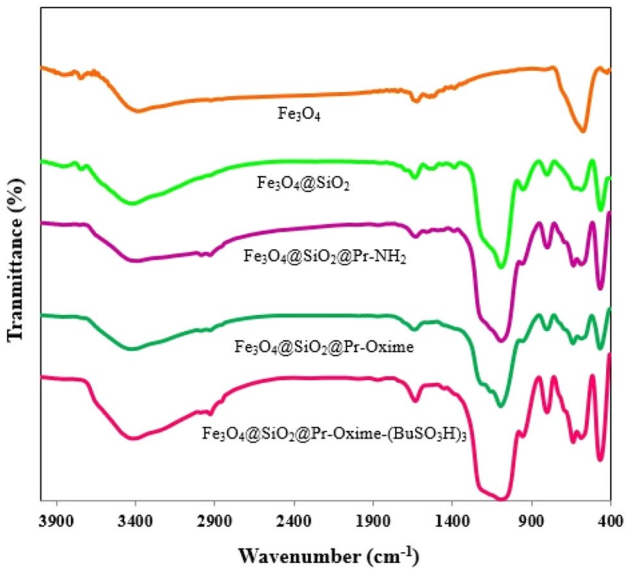

Fig. 1 FTIR spectra of **a** Fe_3O_4, **b** Fe_3O_4@SiO_2, **c** Fe_3O_4@SiO_2@Pr-NH_2, **d** Fe_3O_4@SiO_2@Pr-Oxime, and **e** Fe_3O_4@SiO_2@Pr-Oxime-($BuSO_3H$)$_3$.

The XRD of (a) Fe_3O_4 and (b) Fe_3O_4@SiO_2@Pr-Oxime-($BuSO_3H$)$_3$ is shown in Fig. 2, which demonstrated the specific peaks at 2θ= 30.12°, 35°, 43.17°, 53.58°, 57.10°,

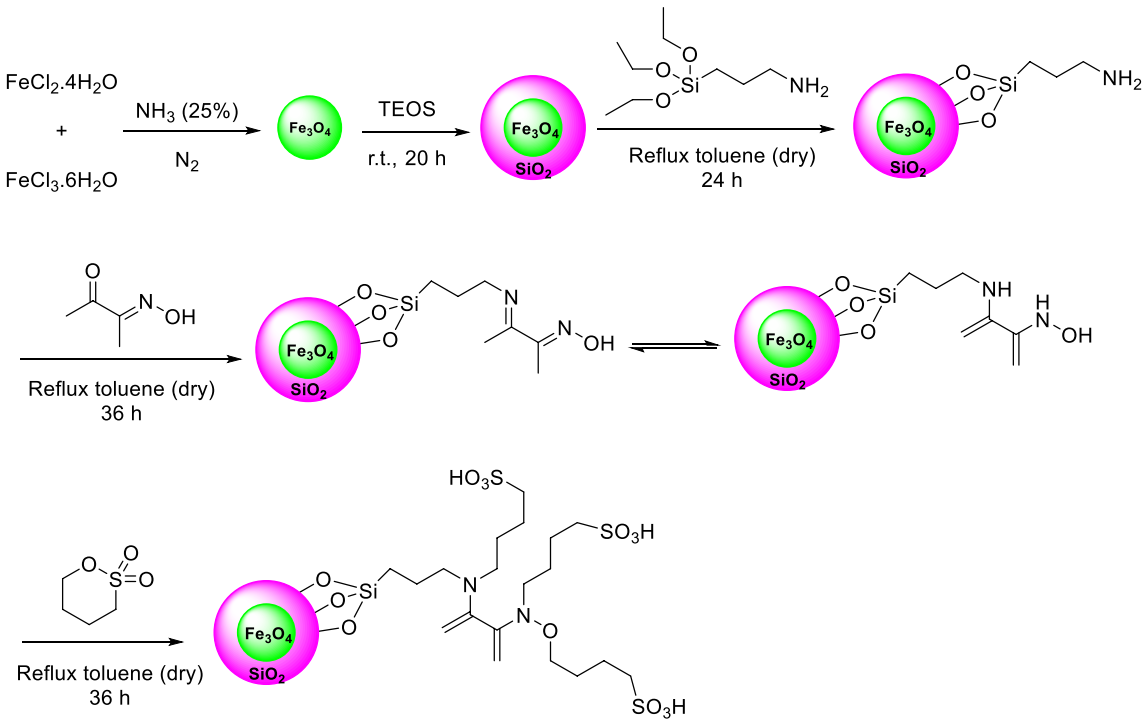

Scheme 2 Synthesis of Fe_3O_4@SiO_2@Pr-Oxime-($BuSO_3H$)$_3$

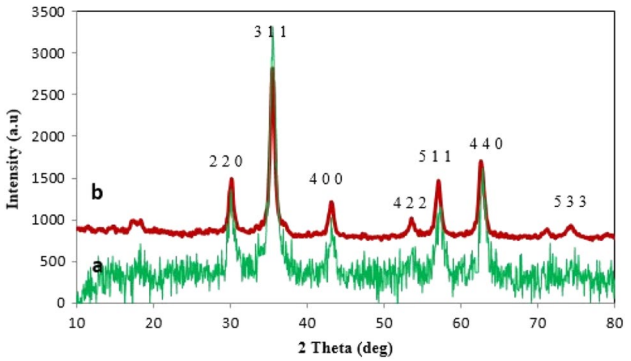

Fig. 2 XRD pattern of **a** Fe_3O_4 and **b**Fe_3O_4@SiO_2@Pr-Oxime-$(BuSO_3H)_3$.

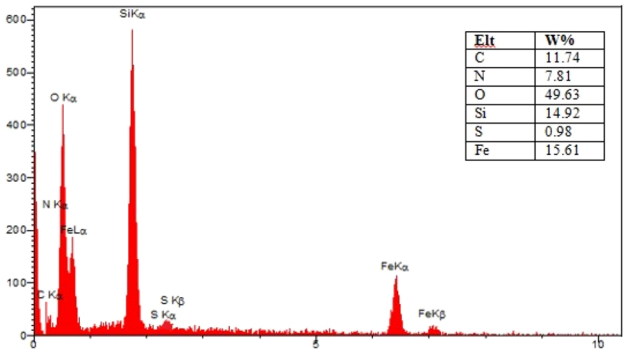

Fig. 3 EDX spectrum of Fe_3O_4@SiO_2@Pr-Oxime-$(BuSO_3H)_3$.

62.65°, and 74.28° corresponding to the (220), (311), (400), (422), (511), (440), and (533) planes.

The EDX analysis of Fe_3O_4@SiO_2@Pr-Oxime-$(BuSO_3H)_3$ is shown in Fig. 3, which demonstrated the different elements such as C, N, O, Si, S, and Fe in the structure of nanocatalyst. The SEM image of Fe_3O_4@SiO_2@Pr-Oxime-$(BuSO_3H)_3$ nanoparticles is shown in Fig. 4, which demonstrated its spherical structure with an average size of 80–100 nm.

The thermal stability of magnetic nanoparticles including Fe_3O_4@SiO_2@Pr-NH_2, Fe_3O_4@SiO_2@Pr-Oxime, and Fe_3O_4@SiO_2@Pr-Oxime-$(BuSO_3H)_3$ was characterized in the range of 25 to 1000 °C as shown in Fig. 5. The mass loss of 2% and 5% was related to the desorption of water on the surface of nanoparticles, which occurred below 200 °C. Also, the decomposition of organic parts occurred in the range of 200–700 °C, which was around 11 %, 21 %, and 26% for Fe_3O_4@SiO_2@Pr-NH_2, Fe_3O_4@SiO_2@Pr-Oxime, and Fe_3O_4@SiO_2@Pr-Oxime-$(BuSO_3H)_3$, respectively. The obtained amount of the organic compound on the nanoparticle surface was about 0.40 mmol g^{-1}.

The magnetic properties of nanoparticles of Fe_3O_4, Fe_3O_4@SiO_2, and Fe_3O_4@SiO_2@Pr-Oxime-$(BuSO_3H)_3$

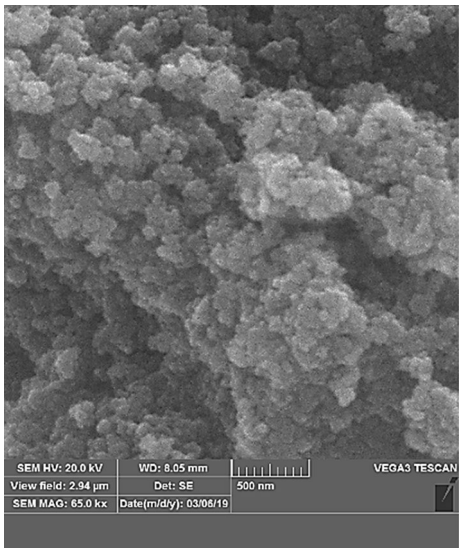

Fig. 4 SEM image of Fe_3O_4@SiO_2@Pr-Oxime-$(BuSO_3H)_3$ nanoparticles.

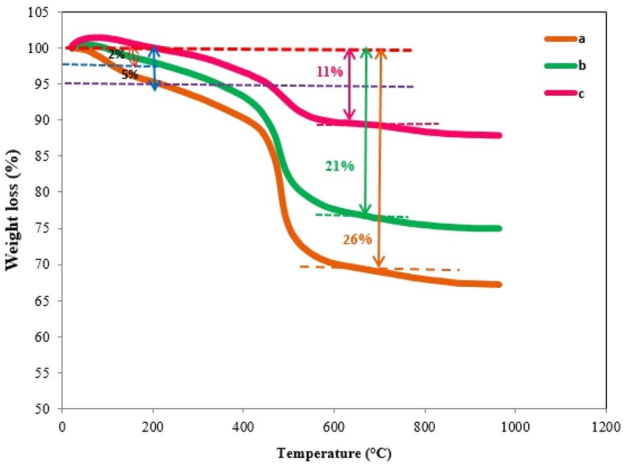

Fig. 5 Thermogravimetric analysis of **a** Fe_3O_4@SiO_2@Pr-Oxime-$(BuSO_3H)_3$, **b** Fe_3O_4@SiO_2@Pr-Oxime, and **c** Fe_3O_4@SiO_2@Pr-NH_2.

were studied by VSM. According to Fig. 6, the magnetization properties of Fe_3O_4, Fe_3O_4@SiO_2, and Fe_3O_4@SiO_2@Pr-Oxime-$(BuSO_3H)_3$ were obtained at about 60 emu/g, 48 emu/g, and 20 emu/g, respectively.

Application of Fe_3O_4@SiO_2@Pr-Oxime-$(BuSO_3H)_3$ in the synthesis of [3.3.3]propellanes

The catalyst activity of Fe_3O_4@SiO_2@Pr-Oxime-$(BuSO_3H)_3$ was investigated for the synthesis of [3.3.3]propellane **5a** as a reaction model (Scheme 3). According to Table 1, the effects of catalyst, solvent, and temperature were studied in the reaction model. Different conditions such as solvent-free

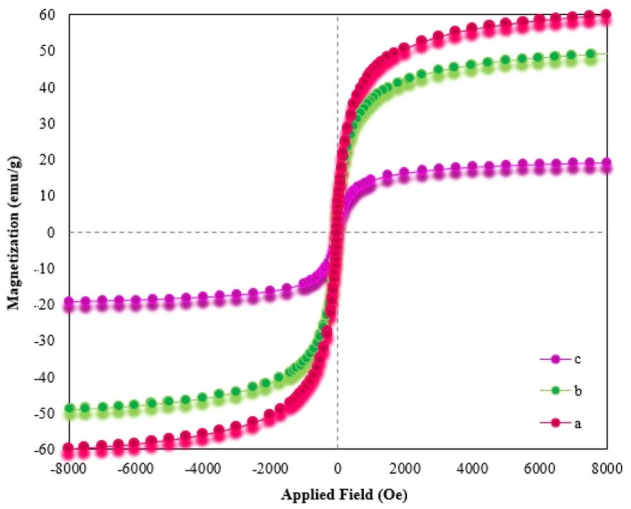

Fig. 6 Magnetization curves of **a** Fe_3O_4, **b** Fe_3O_4@SiO_2, and **c** Fe_3O_4@SiO_2@Pr-Oxime-$(BuSO_3H)_3$

system, reflux in EtOH, H_2O, H_2O/EtOH (1:1), and without a catalyst were tested. Therefore, among the examined conditions, the best result was provided via the domino reaction under the solvent-free condition at 80 °C using Fe_3O_4@SiO_2@Pr-Oxime-$(BuSO_3H)_3$ as nanocatalyst.

The synthesis of [3.3.3]propellane derivatives by Fe_3O_4@SiO_2@Pr-Oxime-$(BuSO_3H)_3$ under the solvent-free conditions at 80°C was studied (Scheme 4). According to Table 2, electron-donor groups such as methyl on the aniline structure led to the increase in the reaction velocity. Therefore, different derivatives of [3.3.3]propellanes were obtained in a high yield and a short reaction time. The new structure was characterized and confirmed by melting point, IR, and ^{1}H NMR spectra.

The possible mechanism for the synthesis of [3.3.3] propellane **5a** by Fe_3O_4@SiO_2@Pr-Oxime-$(BuSO_3H)_3$ is reported in Scheme 2. Initially, carbonyl groups of dimedone **2a** and ninhydrin **3** were protonated in the presence of Fe_3O_4@SiO_2@Pr-Oxime-$(BuSO_3H)_3$ as Brønsted *acid*. Then, the nucleophilic addition of 4-bromoaniline **1a** to protonated dimedone **2a** gave an intermediate **6**. Besides, the Knoevenagel reaction of malononitrile **4** with ninhydrin **3** created intermediate **7**, which was reacted with enamine **6** through the Michael addition to provide intermediate **8**. In the next stage, *via* the proton transfer, intermediate **8** was cyclized, to provide the compound **9**, which was transferred to [3.3.3]propellane **5a** *via* intramolecular O-cyclization and tautomerization reaction (Scheme 5).

Fe_3O_4@SiO_2@Pr-Oxime-$(BuSO_3H)_3$ nanoparticles were washed several times with hot EtOH, distilled water, and diluted sulfonic acid solution and dried. Then, it was applied in the reaction model for four times as given in Table 3.

According to Table 4, the catalyst activity of Fe_3O_4@SiO_2@Pr-Oxime-$(BuSO_3H)_3$ toward other reported conditions was compared. This work has advantages including excellent yields, simple work-up, ecofriendly, purity products, short reaction time, and green condition. Also, the nanomagnetic catalyst was separated from the mixture by the magnet.

Conclusions

In summary, Fe_3O_4@SiO_2@Pr-Oxime-$(BuSO_3H)_3$ as a nanomagnetic catalyst was synthesized and characterized by different techniques such as EDS, VSM, SEM, and XRD. In the following, its catalytic activity was investigated in the synthesis of [3.33]propellanes in good yield and short reaction time.

Table 1 The reaction condition optimization in the synthesis of [3.3.3]propellane **5a**.

Entry	Catalyst (gr)	Solvent	Condition	Time (h)	Yield (%)
1	–	–	r.t.	5	–
2	Cat (0.01)	EtOH	Reflux	4	70
3	Cat (0.01)	H_2O	Reflux	5	50
4	Cat (0.01)	H_2O:EtOH	Reflux	4	60
5	Cat (0.008)	–	80 °C	50 min	90
6	Cat (0.01)	–	80 °C	35 min	92
7	Cat (0.01)	–	100 °C	35 min	50

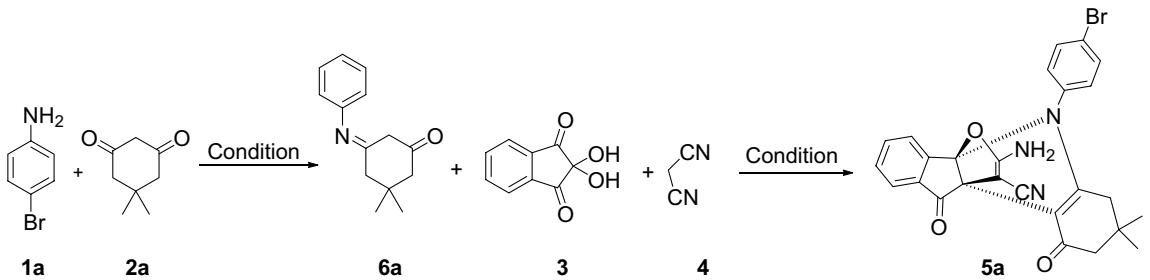

Scheme 3 Synthesis [3.3.3]propellane **5a** as a reaction model

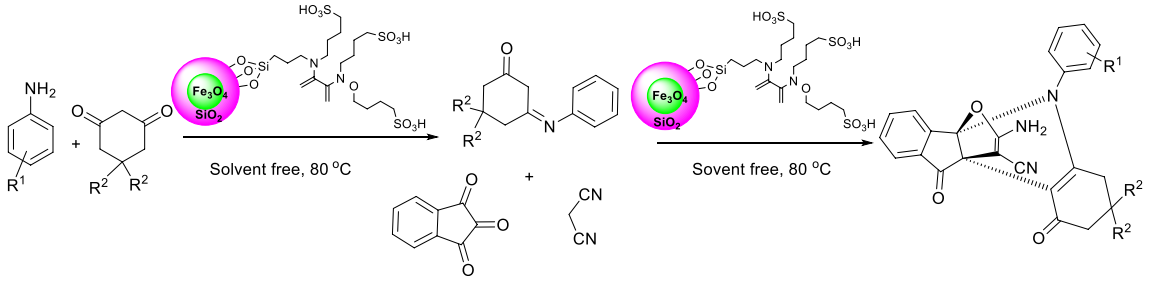

Scheme 4 Synthesis [3.3.3]propellane derivatives **5a–k**.

Table 2 The synthesis of [3.3.3] propellane derivatives **5a–k**.

Entry	R^1	R^2	Number	Time (min)	Yield (%)	m.p (°C)	m.p (°C) [Ref.]
1	4-Br	Me	**5a**	35	92	241-245	238-236 [47]
2	4-Cl	Me	**5b**	35	91	234-236	222-224 [48]
3	2-Cl	Me	**5c**	35	90	227-229	223-226 [48]
4	4-Br	H	**5d**	35	89	240-242	245-246 [47]
5	H	H	**5e**	30	90	227-230	218-220 [44]
6	4-Cl	H	**5f**	35	88	233-235	236-238 [44]
7	4-Me	Me	**5g**	30	93	225-227	220-222 [44]
8	4-NO_2	Me	**5h**	40	88	210-213	214-216 [48]
9	4-Me	H	**5i**	30	90	225-270	222-224 [44]
10	4-NO_2	H	**5j**	40	87	236-240	247-249 [44]
11	3,4-Me_2	H	**5k**	30	95	233-235	New

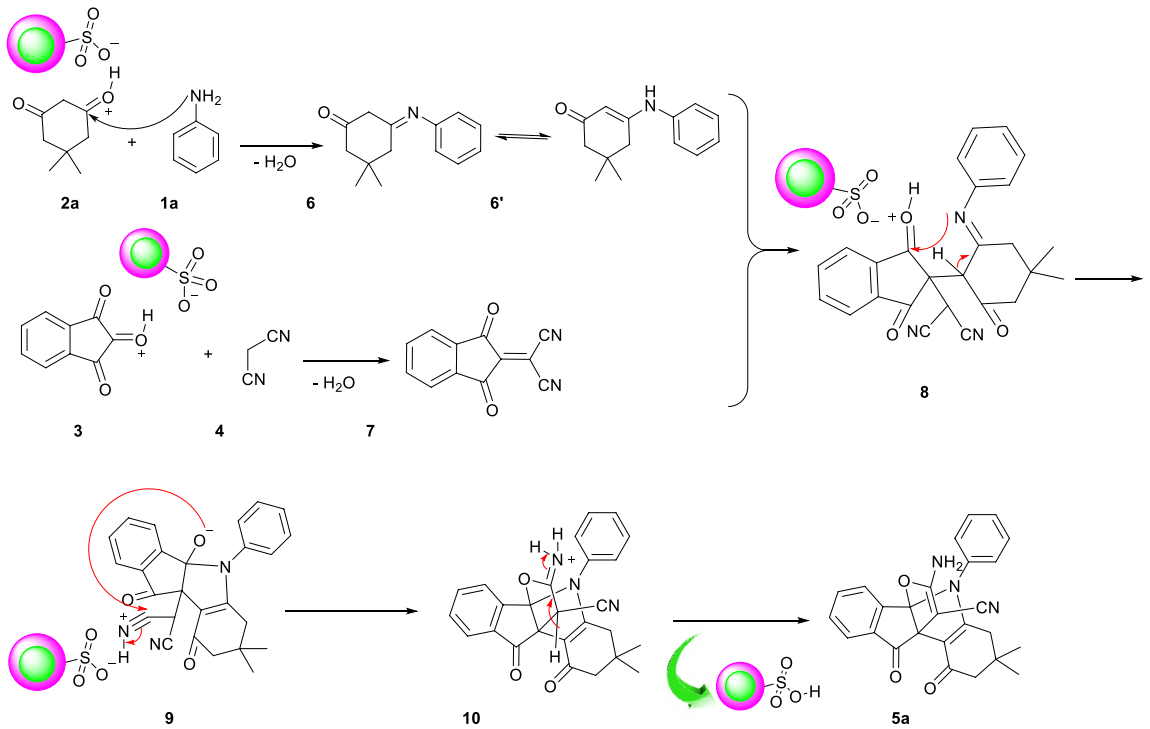

Scheme 5 Synthesis of [3.3.3]propellane **5a**.

Table 3 The reusability of Fe_3O_4@SiO_2@Pr-Oxime-$(BuSO_3H)_3$

Entry	Time (min)	Yield (%)
1	35	92
2	35	90
3	35	88
4	35	84

Table 4 Comparison of reported conditions in the synthesis of compound **5a**.

Entry	Catalyst	Solvent	Condition	Time (h)	Yield (%)
1	Et_3N	EtOH	r.t.	2	78 [36]
2	L-Proline	EtOH	r.t.	4	84 [47]
3	CSB-Ni(II)	EtOH	r.t.	2.5	79 [48]
4	Fe_3O_4@SiO_2@Pr-Oxime-$(BuSO_3H)_3$	–	80 °C	35 min	92

Supplementary Information The online version contains supplementary material available at https://doi.org/10.1007/s13738-022-02685-7.

Acknowledgements We are grateful to the Alzahra University Research Council's support.

References

1. G. Mohammadi Ziarani, M. Khademi, F. Mohajer, M. Anafcheh, A. Badiei, J.B. Ghasemi, Res. Chem. Intermed. **48**, 2111 (2022)
2. B. Tahmasbi, A. Ghorbani-Choghamarani, Catal Lett. **147**, 649 (2017)
3. M. Zarei, H. Sepehrmansourie, M.A. Zolfigol, R. Karamian, S.H.M. Farida, New J Chem. **42**, 14308 (2018)
4. L. Zhao, X. Song, X. Ouyang, J. Zhou, J. Li, D. Deng, ACS Appl. Mater. Interfaces **13**, 49631 (2021)
5. G. Mohammadi Ziarani, P. Mofatehnia, F. Mohajer, A. Badiei, RSC Adv. **10**, 30094 (2020)
6. S. Altaf, Z. Rabeea, Q.Z. Waqas, A. Shakil, Y. Khurram, S. Asad, J.K. Asim, B. Muhammad, A. Muhammad, Ecotoxicol. Environ. Saf. **226**, 112826 (2021)
7. J. Lu, Y. Li, H. Zhu, G. Shi, ACS Appl. Nano Mater. **4**, 7856 (2021)
8. L. Xu, Q. Ding, Anal. Methods. **13**, 5487 (2021)
9. H.R. Pouretedal, Z. Bashiri, M. Nasiri, A. Arab, Part. Sci. Technol. **39**, 971 (2021)
10. M. Cohen-Erner, R. Khandadash, R. Hof, O. Shalev, A. Antebi, A. Cyjon, D. Kanakov, A. Nyska, G. Goss, J. Hilton, D. Peer, ACS Appl. Nano Mater. **4**, 11187 (2021)
11. C. Caizer, M. Rai, *Magnetic nanoparticles in alternative tumors therapy: biocompatibility, toxicity, and safety compared with classical methods magnetic nanoparticles in human health and medicine: current medical applications and alternative therapy of cancer* (Wiley, 2021)
12. H. Karimi-Maleh, F. Karimi, Y. Orooji, G. Mansouri, A. Razmjou, A. Aygun, F. Sen, Sci. Rep. **10**, 11699 (2020)
13. H. Karimi-Maleh, B.G. Kumar, S. Rajendran, J. Qin, S. Vadivel, D. Durgalakshmi, F. Gracia, M. Soto-Moscoso, Y. Orooji, F. Karimi, J. Mol. Liq. **314**, 113588 (2020)
14. A. Lascu, *ARKIVOC* 2020, i, **272**, (2020).
15. V. Polshettiwar, R. Luque, A. Fihri, H. Zhu, M. Bouhrara, J.M. Basset, Chem Rev. **111**, 3036 (2011)
16. D. Wang, D. Astruc, Chem Rev. **114**, 6949 (2014)
17. J. Meurig Thomas, R. Raja, Rev. Mater. Res. **35**, 315 (2005)
18. M.J. Yao, Z. Guan, Y.H. He, Synth. Commun. **43**, 2073 (2013)
19. Z. Nezafat, M. Nasrollahzadeh, J. Mol. Struct. **1228**, 129731 (2021)
20. R.W. Weber, J.M. Cook, Can. J. Chem. **56**, 189 (1978)
21. L. Zu, B.W. Boal, N.K. Garg, J. Am. Chem. Soc. **133**, 8877 (2011)
22. J.M. Huang, R. Yokoyama, C.S. Yang, Y. Fukuyama, A. Merrilactone, Tetrahedron Lett. **41**, 6111 (2000)
23. Y. Sugimoto, H.A.A. Babiker, T. Saisho, T. Furumoto, S. Inanaga, M. Kato, J. Org. Chem. **66**, 3299 (2001)
24. K. Weinges, P. Günther, W. Kasel, G. Hubertus, P. Güinther, Angew. Chem. **20**, 960 (1981)
25. M. Konishi, H. Ohkuma, T. Tsuno, T. Oki, G.D. VanDuyne, J. Clardy, J. Am. Chem. Soc **112**, 3715 (1990)
26. B.-W. Yu, J.-Y. Chen, Y.-P. Wang, K.-F. Cheng, X.-Y. Li, G.-W. Qin, Phytochemistry **61**, 439 (2002)
27. G.A. Ellestad, M.P. Kunstmann, H.A. Whaley, E.L. Patterson, J. Am. Chem. Soc. **90**, 1325 (1968)
28. J. Dugan, P. De Mayo, M. Nisbet, J. Robinson, M. Anchel, J. Am. Chem. Soc. **88**, 2838 (1966)
29. A. Rezvanian, A. Alizadeh, L.-G. Zhu, Synlett **23**, 2526 (2012)
30. A. Rezvanian, A. Alizadeh, Tetrahedron **68**, 10164 (2012)
31. A.M. Dilmaç, T. Wezeman, R.M. Bär, S. Bräse, Nat. Prod. Rep. **37**, 224 (2020)
32. A.M. Dilmaç, E. Spuling, A. de Meijere, S. Bräse, Chem. Int. Ed. **56**, 5684 (2017)
33. J.C. Leung, A.A. Bedermann, J.T. Njardarson, D.A. Spiegel, G.K. Murphy, N. Hama, J.L. Wood, Angew. Chem. Int. Ed. **57**, 1991 (2018)
34. K. Kumaravel, G. Vasuki, Curr. Org. Chem. **13**, 1820 (2009)
35. V.K. Ahluwalia, R.S. Varma, *Green solvents for organic synthesis* (Alpha Science International, 2009)
36. L.J. Zhang, C.G. Yan, Tetrahedron **69**, 4915 (2013)
37. A. Alizadeh, A. Rezvanian, L.G. Zhu, J. Org. Chem. **77**, 4385 (2012)
38. I. Yavari, A. Malekafzali, S. Skoulika, Tetrahedron Lett. **55**, 3154 (2014)
39. Z. Kheilkordi, G. Mohammadi Ziarani, A. Badiei, Polyhedron **178**, 114343 (2020)
40. G. Mohammadi Ziarani, Z. Kheilkordi, F. Mohajer, A. Badiei, R. Luque, RSC Adv. **11**, 17456 (2021)
41. Z. Kheilkordi, G. Mohammadi Ziarani, F. Mohajer, J. Iran. Chem. Soc. **17**, 247 (2020)
42. Z. Kheilkordi, G. Mohammadi Ziarani, S. Bahar, A. Badiei, J. Iran. Chem. Soc. **16**, 365 (2019)
43. Z. Kheilkordi, G. Mohammdi Ziarani, N. Lashgari, A. Badiei, Polyhedron **166**, 203 (2019)
44. S. Mahmoudi-GomYek, D. Azarifar, M. Ghaemi, H. Keypour, M. Mahmoudabadi, Appl. Organomet. Chem. **33**, e4918 (2019)
45. M. Rajabi-Salek, M.A. Zolfigol, M. Zarei, Res. Chem. Intermed. **44**, 5255 (2018)
46. A.R. Hajipour, M. Karimzadeh, S. Jalilvand, H. Farrokhpour, A.N. Chermahini, Comput. Theor. Chem. **1045**, 10 (2014)
47. L. Fu, W. Lin, Z.B. Huang, D.Q. Shi, J. Heterocycl. Chem. **52**, 1075 (2015)
48. H. Naeimi, S. Lahouti, Appl. Organomet. Chem. **31**, e3732 (2017)

Springer Nature or its licensor (e.g. a society or other partner) holds exclusive rights to this article under a publishing agreement with the author(s) or other rightsholder(s); author self-archiving of the accepted manuscript version of this article is solely governed by the terms of such publishing agreement and applicable law.